Published in final edited form as:
Inorg Chem. 2010 June 21; 49(12): 5368–5370. doi:10.1021/ic100825x.

Monooxo Molybdenum(VI) Complexes Possessing Olefinic Dithiolene Ligands: Probing Mo-S Covalency Contributions to Electron Transfer in DMSO Reductase Family Molybdoenzymes

Hideki Sugimoto[*,†], **Susumu Tatemoto**[†], **Koichiro Suyama**[‡], **Hiroyuki Miyake**[‡], **Regina P. Mtei**[∫], **Shinobu Itoh**[*,†], and **Martin L. Kirk**[*,∫]

[†]Department of Material and Life Science, Graduate School of Engineering, Osaka University, 2-1, Yamadaoka, Suita, Osaka 565-0871, Japan

[‡]Department of Chemistry, Graduate School of Science, Osaka City University, 3-3-138 Sumiyoshi-ku, Osaka 565-8585, Japan

[∫]Department of Chemistry and Chemical Biology, The University of New Mexico, MSC03 2060, 1 University of New Mexico, Albuquerque, New Mexico 87131-0001

Abstract

A monooxo Mo(VI) model complex for the oxidized active site in the DMSOR family of molybdoenzymes has been synthesized and structurally characterized. The compound was obtained from the desoxo Mo(IV) derivative by clean oxygen atom transfer from an amine *N*–oxide in a manner similar to that observed in the enzyme. A combination of electronic absorption and resonance Raman spectroscopies, coupled with the results of bonding and excited state calculations, has been used to provide strong support for a highly covalent Mo(d_{xy})-S(dithiolene) **π*** bonding interaction in the Mo(VI) complex. It is proposed that the resulting Mo-S covalency facilitates electron transfer regeneration of the catalytically competent DMSOR Mo(IV) active site.

The dimethylsulfoxide reductases (DMSORs) and trimethylamine *N*–oxide reductase (TMAOR) are pyranopterin–containing molybdenum enzymes that catalyze the reduction of Me_2SO and Me_3NO to Me_2S and Me_3N, respectively, and serve as terminal electron acceptors during anaerobic growth of bacteria.[1,2] In the oxidative half reaction, a 5-coordinate desoxo Mo(IV) center abstracts an oxygen atom from the substrate, yielding the reduced product and a 6-coordinate Mo(VI) center that is coordinated by a terminal oxo, a serinate oxygen, and the olefinic dithiolene chelates of two pyranopterin cofactors (Fig. 1).[3] The absorption spectrum of the oxidized Mo(VI) site in DMSOR ($DMSOR_{ox}$) is dominated by low-energy ligand-to-metal charge transfer (LMCT) transitions at ~14000 and ~18300 cm^{-1} that arise from covalent interactions between the Mo(VI) center and the dithiolene donors.[4] The resonance Raman (rR) spectrum of $DMSOR_{ox}$ reveals two ν(C=C) stretches at 1578 and 1527 cm^{-1}, and this is consistent with crystallographic results that show the two

[*]To whom correspondence should be addressed. sugimoto@mls.eng.osaka-u.ac.jp, shinobu@mls.eng.osaka-u.ac.jp, mkirk@unm.edu.

Supporting Information Available: Designation of complexes, experimental details, spectroscopic and crystallographic data, relevant M.O.'s and EDDM's. This material is available free of charge via the Internet at http://pubs.acs.org

dithiolene chelates to be inequivalent.[5] The bis-dithiolene coordination in oxidized DMSOR family has been suggested to modulate the redox potential of the active site, facilitate electron transfer (ET) for regeneration of the Mo(IV) center, and activate the active site for oxygen atom transfer via the entatic principle.[6-8] As such, mono-oxo Mo(VI) model compounds that possess bis-dithiolene ligation and a 6-coordinate distorted octahedral coordination geometry provide much needed benchmarks for understanding the relationship between the catalytic mechanism and active site geometric and electronic structures.[9,10]

Square pyramidal desoxo molybdenum(IV) complexes coordinated by olefinic dithiolene ligands have been prepared by Holm *et al*., and serve as symmetrized structural and functional analogues for the Mo(IV) center found in reduced DMSOR ($DMSOR_{red}$) and other members of the DMSOR enzyme family.[11] However, the mono-oxo molybdenum(VI) species that arise from oxygen atom transfer reactions were too unstable for isolation and full characterization.[11] A mono-oxo molybdenum(VI) bis-dithiolene complex that possesses aromatic dithiolenes has been synthesized, but the corresponding desoxo Mo(IV) compound does not promote clean oxygen atom abstraction.[12,13] We have now synthesized new $[Mo^{VI}O(OSiR_3)(dithiolene)_2]^-$ complexes, that possess biologically relevant olefinic dithiolenes, from their desoxo Mo(IV) derivatives by a clean oxygen atom transfer reaction. The Mo(VI) complexes are 6-coordinate and represent excellent structural and reactivity mimics of the oxidized DMSOR family. The ability to compare enzyme and model spectroscopic data provides insight into oxidized DMSOR family active site electronic structure and covalency contributions to ET.

The desoxo Mo(IV) complexes $[Mo(OSiR_3)(S_2C_2(COOMe)_2)_2]^-$ $\mathbf{1^{OSiR3}}$ (R_3 = $^{i}Pr_3$ ($\mathbf{1^{OSiPr3}}$), $^{t}BuPh_2$ ($\mathbf{1^{OSiBuPh2}}$), $S_2C_2(COOMe)_2$ = 1,2-dicarbomethoxyethylene-1,2-dithiolate, (Chart S1) were prepared from $(Et_4N)_2[Mo^{IV}O(S_2C_2(COOMe)_2)_2]$[14] and the corresponding chlorosilanes. The Mo(IV) center of $\mathbf{1^{OSitBuPh2}}$ exhibits a square pyramidal geometry with the $OSi^{t}BuPh_2$ group coordinated axially (Fig. 2a). The C=C (1.339(3) and 1.332(3) Å) and C-S (mean 1.758(2) Å) bond lengths support an ene-1,2-dithiolate ligand structure as found in all square pyramidal $[Mo^{IV}(OR)(S_2C_2R_2)]^-$ (R = H, Me, Ph) complexes.[11,12,15,16]

Compounds $\mathbf{1^{OSiR3}}$ reacted smoothly with Me_3NO to give a deep-purple solution, although the corresponding reaction with Me_2SO was too slow to be followed. IR spectra of the reaction mixture with Me_3NO show appearance of a new band at 880 cm^{-1} assigned as the ν(Mo≡O) stretch (Fig. S1). Fig. 3 shows a time dependent spectral change of $\mathbf{1^{OSiBuPh2}}$ by a treatment with Me_3NO, where clear isosbestic points are observed at 351 and 316 nm, indicating $\mathbf{1^{OSiR3}}$ exhibits clean oxygen atom transfer. The oxygen atom transfer reaction was analyzed kinetically to give parameters of k^{258} = 5.68 M^{-1} s^{-1}, $\Delta H^{\ddagger}$ = 8.5 (kcal mol^{-1}), and $\Delta S^{\ddagger}$ = −15 (eu). (see Figures S2 – S3). Purple species generated from $\mathbf{1^{OSiR3}}$ and Me_3NO were stable enough for isolation, $[Mo^{VI}O(OSiR_3)(S_2C_2(COOMe)_2)_2]^-$ ($\mathbf{2^{OSiR3}}$), and the crystal structure of $\mathbf{2^{OSiPr3}}$ is depicted in Fig. 2b. Compound $\mathbf{2^{OSiPr3}}$ possesses a distorted octahedral structure with a S1-S2-S3-S4 dihedral angle of 108°. The terminal oxo exerts a strong *trans* influence on the Mo-S4 bond, resulting in a long Mo-S4 bond distance (2.5607(8) Å) when compared to the three *cis* Mo-S bonds (mean 2.431(1) Å), and this underscores a key difference between the two dithiolenes present in $\mathbf{2^{OSiPr3}}$.

The solution electronic absorption spectrum of **2**$^{\mathbf{OSiPr3}}$ (Fig. 4) is remarkably similar to that of $DMSOR_{ox}$ displaying two low energy bands at 13533 cm^{-1} (ε = 1350 $M^{-1}cm^{-1}$) and 17549 cm^{-1} (ε = 2800 $M^{-1}cm^{-1}$).[4] The rR data for **2**$^{\mathbf{OSiPr3}}$ show two dithiolene C=C stretches at 1554 and 1489 cm^{-1} which are also in good agreement with the enzyme data (Figure 5b), *vide supra*. The latter value is close to that observed in its dioxo molybdenum(VI) analogue (1494 and 1510 cm^{-1}), $(Et_4N)_2[MoO_2(S_2C_2(COOMe)_2)_2]^{2-}$.[17] Further, vibrational frequency calculations performed on a model for **2**$^{\mathbf{OSiPr3}}$ show C=C stretching modes at 1577 and 1505 cm^{-1} that derive from dithiolene A and B respectively (see Fig. 2). On the other hand, a single C=C stretch is observed at 1550 cm^{-1} for **1**$^{\mathbf{OSiBuPh2}}$ (Fig. 5a).[18] The rR data underscore the marked inequivalence of the two dithiolenes in **2**$^{\mathbf{OSiPr3}}$ with respect to their bonding interactions with the Mo center.

Our bonding and excited state calculations strongly support an argument whereby the *cis* $S(p_z)$ orbital associated with dithiolene (B) acts as an acceptor in the low-energy LMCT transitions (Fig. 4) Thus, we can assign Band 1 as a HOMO→LUMO transition that displays considerable dithiolene (A)→$Mo(d_{xy})$ CT character (Fig. 4, inset).[19] This derives from the fact that the LUMO is dominantly $Mo(d_{xy})$-dithiolene (B) in character while the HOMO possesses nearly equal contributions from both dithiolenes. Band 2 is assigned as a dithiolene (A+B)→$Mo(d_{xy})$ CT transition with dominant HOMO-1→LUMO character (Figs. 6 and S5). Interestingly, the distorted O_h geometry of **2**$^{\mathbf{OSiPr3}}$ results in a LUMO wavefunction that possesses a strong π^* interaction between the *cis* $S(p_z)$ orbital localized on dithiolene (B) and the $Mo(d_{xy})$ orbital (Fig. 6). We previously observed a similar Mo-S π^* bonding interaction resulting in a large Mo-S covalency and an intense $S_{thiolate}$→$Mo(d_{xy})$ CT transition in oxomolybdenum thiolate complexes.[20] The high Mo-S covalency was observed to be a direct result of an ~180° O_{oxo}-Mo-S-C dihedral angle involving one of the thiolate donors. This geometry properly orients a S(p) orbital for maximum π overlap with the Mo(xy) orbital, resulting in a bonding scheme similar to that observed in blue copper proteins.[21] A 176° O_{oxo}-Mo-$S_{dithiolene}$-C dihedral angle involving a single S donor on dithiolene B is present in **2**$^{\mathbf{OSiPr3}}$. This results in the *cis* S donor of dithiolene B contributing ~18% S character to the LUMO wavefunction, which is approximately half that found for the blue copper site (~35%).[21] The implication here is that the Mo(xy) redox orbital in $DMSOR_{ox}$ possesses a strong π-type bonding interaction with a single $S_{dithiolene}$ donor, and this is anticipated to provide a covalent pathway for electron transfer regeneration of the $DMSOR_{red}$ site.

In summary, **2**$^{\mathbf{OSiR3}}$ are monooxo Mo(VI) complexes that coordinate olefinic dithiolene ligands in a manner similar to the Mo active site in oxidized DMSOR family. The complexes can be generated from **1**$^{\mathbf{OSiR3}}$ by clean oxygen atom transfer in a manner similar to that observed in the enzymes. A combination of crystallography and electronic absorption and rR spectroscopies strongly supports a unique bonding interaction in **2**$^{\mathbf{OSiPr3}}$ and, by inference, $DMSOR_{ox}$. Low-energy LMCT transitions to a LUMO acceptor orbital that possesses considerable $Mo(d_{xy})$-$S_{dithiolene}$ π^* character have been assigned. We suggest that the $Mo(d_{xy})$-$S_{dithiolene}$ π^* bonding interaction found in **2**$^{\mathbf{OSiPr3}}$ may play a key role in facilitating ET regeneration of the $DMSOR_{red}$ site. This would occur by coupling the Mo center into hole superexchange pathways that involve a single dithiolene ligand which

possesses a S donor ligand *cis* to the Mo≡O bond with an ~180° O_{oxo}-Mo-$S_{didthiolene}$-C dihedral angle as observed in **2**$^{\mathbf{OSiPr3}}$.

Supplementary Material

Refer to Web version on PubMed Central for supplementary material.

Acknowledgments

This work was partly supported by a Grant (22108520 to H.S.) for Scientific Research on Priority Areas "Coordination Programming" from MEXT of Japan. M.L.K. acknowledges the National Institutes of Health (GM-057378) for financial assistance.

References

1. Hille R. Chem Rev. 1996; 96:2757. [PubMed: 11848841]
2. Burgmayer SJN. Prog Inorg Chem. 2004; 52:491.
3. Li H-K, Temple C, Rajagopalan KV, Schindelin H. J Am Chem Soc. 2000; 122:7673.
4. Cobb N, Conrads T, Hille R. J Biol Chem. 2005; 280:11007. [PubMed: 15649898]
5. Garton SD, Hilton J, Oku H, Crouse BR, Rajagopalan KV, Johnson MK. J Am Chem Soc. 1997; 119:12906.
6. Kirk ML, Helton ME, McNaughton RL. Prog Inorg Chem. 2004; 52:111.
7. McNaughton RL, Lim BS, Knottenbelt SZ, Holm RH, Kirk ML. J Am Chem Soc. 2008; 130:4628. [PubMed: 18341333]
8. Webster CE, Hall MB. J Am Chem Soc. 2001; 123:5820. [PubMed: 11403624]
9. Enemark JH, Cooney JJA, Wang J-J, Holm RH. Chem Rev. 2004; 104:1175. [PubMed: 14871153]
10. Sugimoto H, Tsukube H. Chem Soc Rev. 2008; 37:2609. [PubMed: 19020675]
11. (a) Lim BS, Holm RH. J Am Chem Soc. 2001; 123:1920. [PubMed: 11456813] (b) Wang J-J, Kryatova OP, Rybak-Akimova EV, Holm RH. Inorg Chem. 2004; 43:8092. [PubMed: 15578849] (c) Wang J-J, Tessier C, Holm RH. Inorg Chem. 2006; 45:2979. [PubMed: 16562954]
12. Donahue JP, Goldsmith CR, Nadiminti U, Holm RH. J Am Chem Soc. 1998; 120:12869.
13. The monooxo molybdenum(VI) complex was prepared from the dioxo Mo(VI) derivative and corresponding chlorosilane.[12].
14. Coucouvanis D, Hadjikyriacou A, Toupadakis A, Koo SM, Ileperuma O, Dragonjac M, Salifoglou A. Inorg Chem. 1991; 30:754.
15. Lim BS, Donahue JP, Holm RH. Inorg Chem. 2000; 39:263. [PubMed: 11272534]
16. Fomitchev DV, Lim BS, Holm RH. Inorg Chem. 2001; 40:645. [PubMed: 11225106]
17. Sugimoto H, Tatemoto S, Suyam K, Miyake H, Itoh S, Dong C, Yang J, Kirk ML. Inorg Chem. 2009; 48:10581. [PubMed: 19831360]
18. The FT Raman of solid **1**$^{\mathbf{OSiBuPh2}}$ exhibited one strong peak assigned as the ν(C=C) stretch at 1548 cm^{-1} (Figure S4). High moisture sensitivity of **2**$^{\mathbf{OSiR3}}$ prevented Raman spectra in the solid state.
19. Gaussian 03, Revision C.02. Gaussian, Inc.; Wallingford CT: 2004.
20. McNaughton RL, Helton ME, Cosper MM, Enemark JH, Kirk ML. Inorg Chem. 2004; 43:1625. [PubMed: 14989655]
21. Gewirth AA, Solomon EI. J Am Chem Soc. 1988; 110:3811–3819.

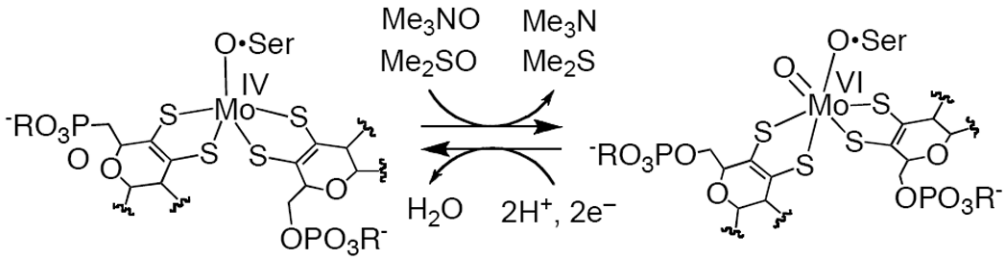

Figure 1.

Representation of the catalytically active desoxo Mo^{IV} and monooxo Mo^{VI} structures in DMSOR and TMAOR of DMSOR family.

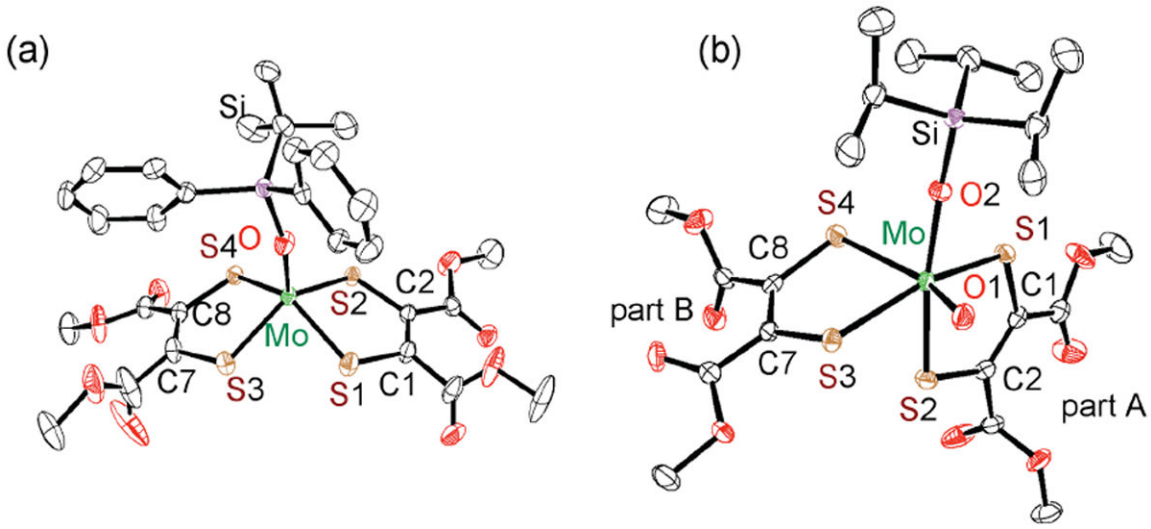

Figure 2.

Crystal structures of complexes $\mathbf{1}^{\mathbf{OSiBuPh2}}$ (a) and $\mathbf{2}^{\mathbf{OSiPr3}}$ (b) with 50% thermal ellipsoids. Selected bond lengths (Å) and angles (°): for $\mathbf{1}^{\mathbf{OSiBuPh2}}$, S1-C1 1.757(2), S2-C2 1.762(2), S3-C7 1.756(2), S4-C8 1.755(2), C1-C2 1.330(3), C7-C8 1.341(3); for $\mathbf{2}^{\mathbf{OSiPr3}}$, Mo-S1 2.4162(9), Mo-S2 2.4778(7), Mo-S3 2.3979(8), Mo-S4 2.5607(8), S1-C1 1.753(3), S2-C2 1.728(3), S3-C7 1.727(3), S4-C8 1.704(3), C1-C2 1.357(4), C7-C8 1.369(4), O1-Mo-S4 156.90(8), O2-Mo-S2 157.89(8).

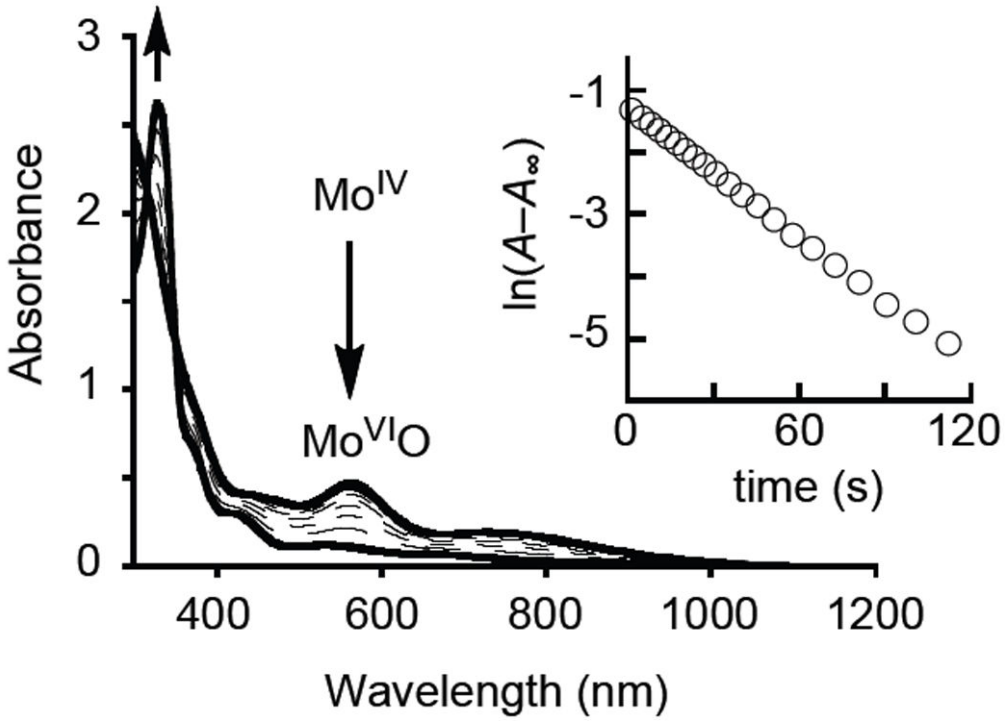

Figure 3.

Spectral change for the oxygen atom transfer from Me_3NO (7.5 mM) to **1**$^{\mathbf{OSiBuPh2}}$ (0.15 mM) in CH_3CN at 253 K. (Inset) First-order plot based on the decrease of absorption at 563 nm.

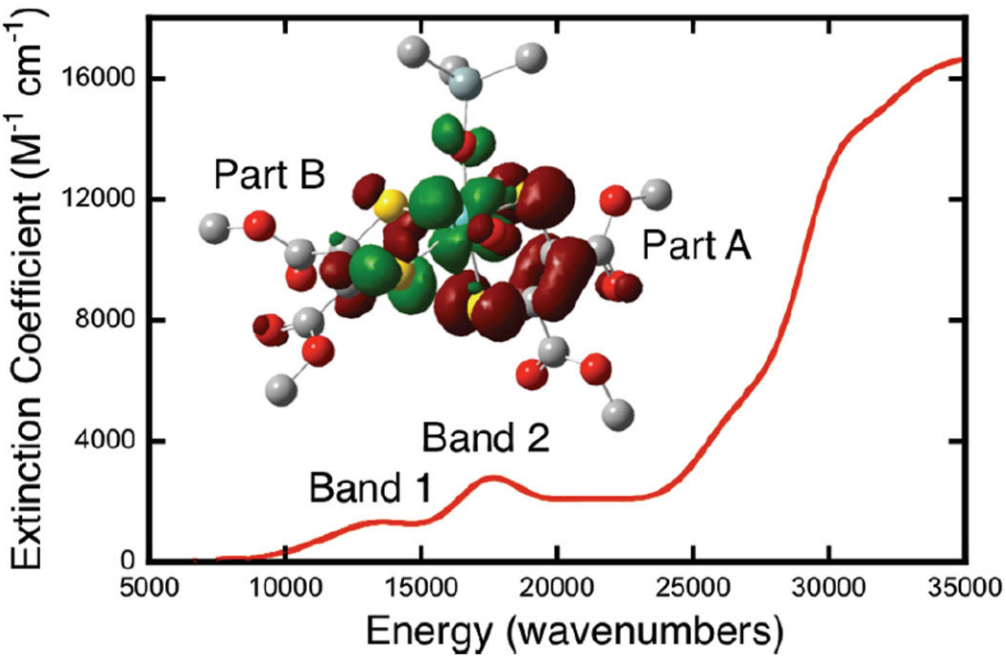

Figure 4.

Solution electronic absorption spectrum of **2**$^{\mathbf{OSiPr3}}$. Inset: Electron density difference map for the transition responsible for Band 1. Red indicates a loss of electron density in the transition and green indicates a gain in electron density.

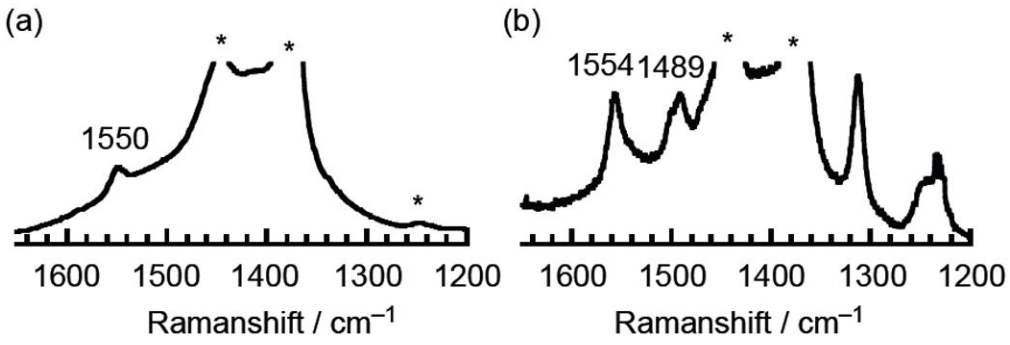

Figure 5.

Resonance Raman spectra of complexes, (a) $\mathbf{1}^{\mathbf{OSiBuPh2}}$ (8.6×10^{-3} M) and (b) $\mathbf{2}^{\mathbf{OSiPr3}}$ (2.3×10^{-3} M) in CH_3CN with excitation at 632.8 nm. Asterisks indicate solvent peaks.

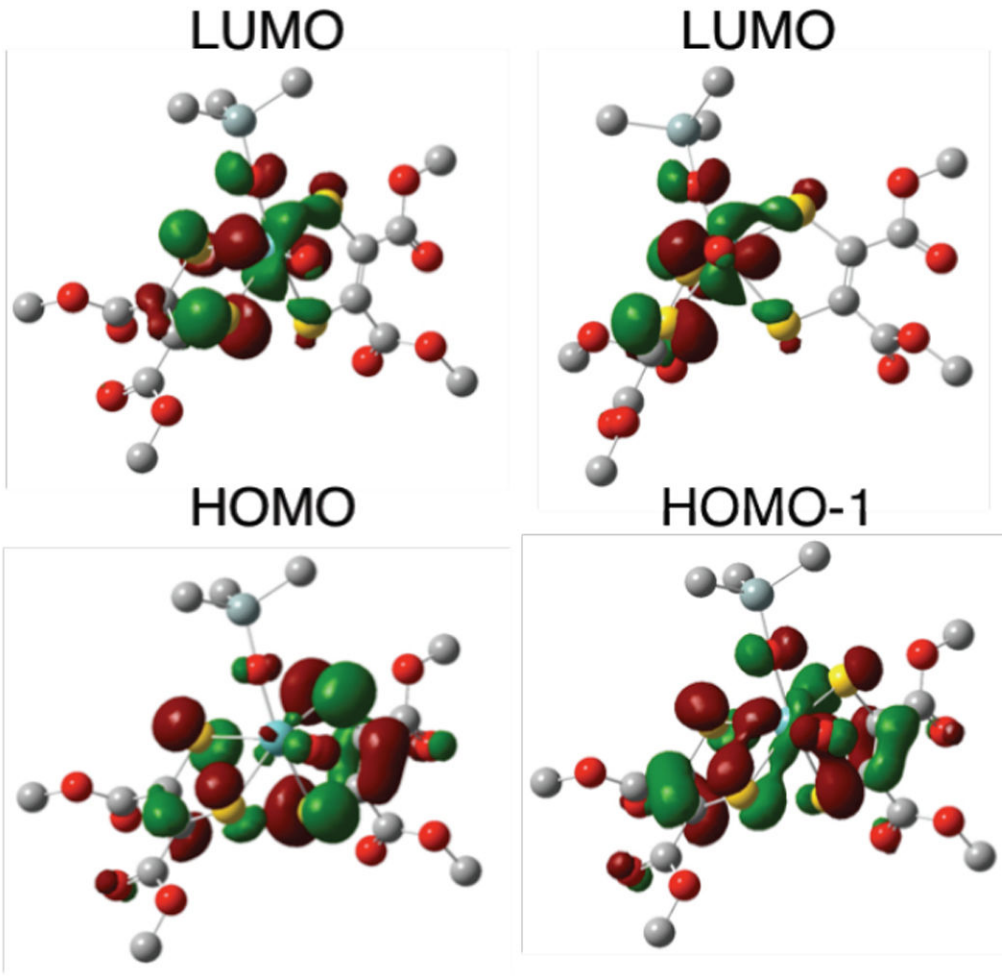

Figure 6.

Kohn-Sham orbitals representing relevant molecular orbitals for **2**. LUMO orientation in upper right hand corner is projected down the Mo≡O bond. In this projection, the LUMO wavefunction is observed to possesses a strong Mo(d_{xy})-S(p_z) **π*** interaction involving the *cis* S(p_z) orbital on the B dithiolene.